

1 **Capturing the spatial variability of algal bloom development in a shallow temperate lake**

2 **Authors:** David Ortiz<sup>1,2\*</sup>, Grace Wilkinson<sup>1,2</sup>

3 <sup>1</sup>Department of Ecology, Evolution, and Organismal Biology, Iowa State University, Ames,  
4 Iowa USA 50010

5 <sup>2</sup>Current Address: Center for Limnology, University of Wisconsin – Madison, Madison,  
6 Wisconsin USA 53706

7 \*Corresponding Author: dortiz4@wisc.edu

8

9 **Keywords:** spatial heterogeneity, spatial analysis, rarefaction analysis, macrophytes, eutrophic

10

11 This manuscript has been submitted for publication in *Freshwater Biology*. Please note that, despite having  
12 undergone peer review, the manuscript has yet to be formally accepted for publication. Subsequent versions of this  
13 manuscript may have slightly different content. If accepted, the final version of this manuscript will be available via  
14 the 'Peer-reviewed Publication DOI' link on the right-hand side of this webpage. Please feel free to contact any of  
15 the authors; we welcome feedback.

## 16 Abstract

- 17 1. Algal blooms can have profound effects on the structure and function of aquatic  
18 ecosystems and have the potential to interrupt valuable ecosystem services. Despite the  
19 potential ecological and economic consequences of algal blooms, the spatial dynamics of  
20 bloom development in spatially complex ecosystems such as shallow lakes remain poorly  
21 characterized. Our goal was to evaluate the magnitude and drivers of spatial variability of  
22 algal biomass, dissolved oxygen and pH over the course of a season, in a shallow lake in  
23 order to better understand the spatial dynamics of algal blooms in these ecosystems.
- 24 2. We sampled 98 locations in a small eutrophic lake on a 65m grid for several parameters  
25 (chlorophyll *a*, phycocyanin, dissolved oxygen, pH, and temperature), weekly over 122  
26 days. This was done to estimate the dynamics of variability and spatial autocorrelation  
27 during the course of multiple bloom events. We also compared the spatial measurements  
28 to a high frequency sensor deployed at a fixed station and estimated the optimal spatial  
29 sampling resolution by performing a rarefaction analysis.
- 30 3. Spatial heterogeneity of algal pigments was high, particularly during bloom events, and  
31 this pattern and the overall severity of the bloom was not well captured with the fixed  
32 station monitoring. The pattern of algal pigments and other limnologically important  
33 variables (dissolved oxygen and pH) was related to the direction of prevailing winds 24  
34 hours prior to sampling and likely enhanced by the shallow northern basin of the lake  
35 where the main surface inlet was located. Additionally, a dense bed of floating-leaf  
36 macrophytes contributed to local patchiness in all variables. Finally, from the rarefaction  
37 analysis we found that minimal information about the mean state of the ecosystem was  
38 gained after ~30 locations had been sampled.

39 4. This study revealed how spatially heterogeneous shallow lakes are over the course of a  
40 single season, and that the magnitude of variability was highest during biologically -  
41 intensive periods such as algal blooms. As such, continued research is needed across a  
42 range of trophic conditions to better understand the structure of horizontal variability in  
43 lakes. Overall, these data demonstrate the need for spatially-explicit monitoring to better  
44 understand the dynamics and drivers of algal blooms in shallow lakes and to better  
45 manage ecosystem services.

46 **Introduction**

47           Lakes are highly dynamic ecosystems that can undergo rapid physical and chemical  
48 changes at an individual location, throughout their water column, and across the entire lake  
49 surface at the scale of hours, days, seasons, and years (Laas et al., 2012; Read et al., 2011;  
50 Wynne & Stumpf, 2015). Quantifying heterogeneity in aquatic ecosystem structure and function  
51 not only improves our understanding of lake ecology and the underlying mechanisms that drive  
52 spatial and temporal heterogeneity, but also provides insights that improve management of these  
53 ecosystems and the services they provide. With the development of sophisticated sensor  
54 technology, high frequency measurements of variables such as dissolved oxygen and temperature  
55 have helped limnologists grasp the scale of temporal heterogeneity in lakes (Carpenter et al.,  
56 2020; Chaffin et al., 2020; Cotterill et al., 2019). Detailed temporal monitoring has led to  
57 advances in understanding several lake mechanisms such as diel cycles in primary production  
58 (Solomon et al., 2013; Staehr et al., 2012), temperature effects on biogeochemical processes  
59 (Medeiros et al., 2012), and early warnings of the transition to alternative stable states (Carpenter  
60 et al., 2011; Wilkinson et al., 2018). Additionally, high frequency measurements have been used  
61 to better understand heterogeneity over depth (vertical spatial heterogeneity) for important  
62 processes such as stratification (Boehrer & Schultze, 2008; Read et al., 2011). Despite these  
63 advances in understanding temporal and vertical heterogeneity, less is known about the dynamics  
64 of horizontal spatial heterogeneity in the surface waters of lakes.

65           The vast majority of our understanding of lentic ecosystem structure and function comes  
66 from single station sampling, with measurements taken through time over the deepest point in  
67 the lake (Stanley et al., 2019). This location is usually selected to be representative of conditions  
68 in the lake; however, the representativeness of a single location is likely to vary with regards to

69 the variable being measured and with time due to interacting forces such as wind, hydrology,  
70 bathymetry, and biology (Chaffin et al., 2020; Schilder et al., 2013; Wu et al., 2010; Zhou.,  
71 2013). For example, ecosystem metabolism measured at dozens of locations for 10 days in two  
72 north temperate lakes varied 1-2 orders of magnitude, with more than three-quarters of the  
73 variability attributable to the measurement location within the lake (Van de Bogert et al., 2012).  
74 Transect-based studies of reservoirs have revealed gradients in algae pigments, pH, and nutrients  
75 with differences varying between 25%-180% within a waterbody (Moreno-Ostos et al., 2009;  
76 Rychtecky & Znachor, 2011; Smith, 2018). Recently, satellite-based studies have demonstrated  
77 the ability to detect spatial patterns at a high resolution for optical variables in large lakes (Lekki  
78 et al., 2019). Despite these advances, relatively few studies have quantified horizontal spatial  
79 variability over time in lakes (Buttita et al. 2017, Vilas et al. 2017, Loken et al. 2019), hampering  
80 our understanding of the magnitude of heterogeneity in variables important for managing water  
81 quality and ecosystem services.

82 The development of algal blooms is expected to be a spatially heterogeneous  
83 phenomenon (Buelo et al., 2018; Butitta, Carpenter et al., 2017; Serizawa et al., 2008) due to  
84 both local heterogeneity in nutrient limitation, zooplankton grazing, and temperature (Davis et  
85 al., 2009; Hansen et al., 1997) and population scale heterogeneity due to wind (George &  
86 Heaney, 1978). Algal blooms can have a negative effect on ecosystem services, and therefore are  
87 often a target for ecosystem monitoring and management. Some bloom-forming taxa,  
88 particularly freshwater cyanobacteria, can produce toxins that rise to dangerous concentrations  
89 for humans, pets, and livestock (Codd et al., 2005; Corbel et al., 2014). Additionally, the  
90 mineralization of settling phytoplankton contributes to anoxic bottom waters, while intense  
91 periods of primary production cause large variation in dissolved oxygen and pH (in poorly

92 buffered ecosystems) over the course of the day, which is stressful for aquatic organisms  
93 (Gilbert, 2017; Landsberg, 2002). Furthermore, the perceived recreational value of lakes declines  
94 when blooms form (Angradi et al., 2018), which in turn can negatively affect local economies  
95 (Dodds et al., 2009). Despite the risk of economic loss, loss in biodiversity, and potential human  
96 harm, the spatial dynamics of bloom development in spatially complex ecosystems such as  
97 shallow lakes remain poorly characterized.

98         Shallow lakes have a large interface between the sediment and water relative to deeper  
99 lakes, making them more susceptible to rapid changes in water residence time and nutrient inputs  
100 (Christensen et al., 2013; Rennella & Quiros, 2006; Romo et al., 2013). Due to the expansive  
101 littoral zones, shallow lakes can have large macrophyte beds which modify the light climate and  
102 turbulence at the sediment-water interface (Andersen et al., 2017; Moller & Rordam, 1985; Vilas  
103 et al., 2017). Many shallow lakes are also polymictic, experiencing multiple periods of  
104 stratification followed by mixing during the ice-free season. During periods of water column  
105 stability, some cyanobacteria taxa thrive, initiating blooms (Carey et al., 2012). Additionally,  
106 episodic nutrient loading from the watershed during storm events (Carpenter et al., 2015; Kelly  
107 et al., 2019), spatial gradients in nutrient availability due to stream inlets and morphology (e.g.  
108 embayments), and wind-driven circulation (Schoen et al., 2014) can all contribute to spatial  
109 heterogeneity of algal blooms over time in shallow lakes.

110         In order to better understand the spatial dynamics of algal blooms in shallow lakes, we  
111 performed intensive spatial sampling on Swan Lake (Iowa, USA), a spatially complex, shallow,  
112 hypereutrophic waterbody with a history of toxic cyanobacteria algal blooms. In addition to  
113 measuring algal pigments throughout the lake over the course of 122 days, we also measured  
114 temperature, dissolved oxygen, and pH. The spatial sampling captured two bloom events and

115 coincided with high frequency monitoring of the same variables using autonomous sensors  
116 deployed at a fixed station (Ortiz et al. 2020). Using these data, we addressed the following  
117 questions: 1) how does spatial variability of algae, dissolved oxygen, and pH change over the  
118 course of a season, 2) are high frequency measurements at a fixed station an adequate  
119 characterization of surface water dynamics in a shallow lake, and 3) what is the optimal spatial  
120 sampling frequency to capture the mean state of a productive waterbody? Evaluating these  
121 questions with data from a spatially complex, hypereutrophic lake will provide valuable  
122 ecological and management-relevant insights into algal bloom dynamics.

123

## 124 **Methods**

### 125 *Study Site*

126 Swan Lake (42.0396, -94.8454) has an average depth of 2 m, surface area of 40.5  
127 hectares, and a shoreline development index value of 1.54. The watershed is 350 hectares with  
128 92% of the land in agricultural use. The estimated water residence time is approximately 1.5  
129 years. During the ice-free period of 2018, Swan Lake had an average total phosphorus  
130 concentration of  $280 \mu\text{g L}^{-1}$  and a total nitrogen concentration of  $1.61 \text{ mg L}^{-1}$ , making it  
131 hypereutrophic (Carlson, 1977). Total nitrogen was measured as the sum of total Kjeldahl  
132 nitrogen (method 351.2 v2, US EPA, 1993c) and nitrate + nitrite measured using the cadmium  
133 reduction method (method 4500-NO<sub>3</sub>-F, US EPA, 1993a). Total phosphorus was measured using  
134 the ascorbic acid method (method 365.1 v2, US EPA, 1993b). The average total alkalinity during  
135 the same period was  $139 \text{ mg CaCO}_3 \text{ L}^{-1}$  determined through end point titration (APHA, 1998). In  
136 addition to seasonal algal blooms, Swan Lake also has non-continuous beds of American lotus  
137 (*Nelumbo lutea*) and sago pondweed (*Stuckenia pectinata*) that peak in biomass in the latter half

138 of the summer and then begin senescing. The main surface inlet to the lake enters on the western  
139 side and the outlet is at the southern edge of the waterbody (Figure 1). There are no known  
140 springs feeding the lake.

141

#### 142 *Field Methods*

143 The spatial sampling occurred approximately weekly from day of year (DOY) 142 to  
144 DOY 264, encompassing the late spring, summer, and early autumn. A total of 16 spatial  
145 sampling events occurred over the course of the 122 days. Measurements of chlorophyll *a*,  
146 phycocyanin, temperature, dissolved oxygen saturation and pH were taken 0.25 m below the  
147 surface at 98 sampling stations using a YSI Pro DSS multiparameter sonde (Yellow Springs  
148 Instrument, Yellow Springs, OH) suspended over the side of a 3-meter long jon boat equipped  
149 with an outboard motor. The sensors, which included the fluorometric Total Algae (chlorophyll *a*  
150 and phycocyanin), optical dissolved oxygen, and Ag/AgCl pH sensors, were calibrated weekly  
151 prior to each sampling event according to manufacturer instructions. The sampling stations were  
152 laid out in a 65 x 65 m grid across the lake (Figure 1) with each location measured in the same  
153 order (north to south) for each sampling event. This spatial resolution was selected to allow for  
154 many sampling locations to be measured in a relatively short window of time, thereby  
155 minimizing the chance that the differences observed between sampling locations was not due to  
156 time of day. Measurements were taken between 10:00 and 14:00, except for the first two and last  
157 three weeks when sampling lasted until 16:00. Beginning on DOY 177 when submerged  
158 macrophytes could be identified from the jon boat, the presence or absence of submerged or  
159 floating leaf macrophytes was noted at each sampling station during each sampling event. These  
160 weekly presence/absence data were used to construct the macrophyte distributions in Figure 1 .



161           The fixed station high frequency monitoring of Swan Lake was performed using a YSI  
162 EXO2 (Yellow Springs Instrument, Yellow Springs, OH) multiparameter sonde equipped with  
163 the same sensors as the YSI ProDSS used for the spatial sampling. The sonde recorded  
164 measurements of chlorophyll *a*, phycocyanin, dissolved oxygen saturation, and pH every 15  
165 minutes. The instrument was deployed on DOY 135 over the deepest point in the lake (3.8 m  
166 deep), hanging approximately 0.5m below the surface, and removed on DOY 264 after the  
167 spatial sampling event on that day. The fixed station sonde was monitored weekly for drift and  
168 calibrated according to manufacturer instructions when indicated by the quality control algorithm  
169 in the KorEXO software. Hourly precipitation, wind speed, and wind direction were collected at  
170 the Arthur N. Neu Airport in Carroll, Iowa, located 4.5 km from the lake, as a part of the  
171 National Oceanic and Atmospheric Automated Surface Observatory System. The meteorological  
172 data were used to aid in the interpretation of spatial dynamics over the course of the summer.

173

#### 174 *Data analysis*

175           Spatial heterogeneity can be quantified by calculating the spatial variance (e.g.,  
176 coefficient of variation; CV) or spatial autocorrelation (Moran's I, Moran, 1950). Increasing  
177 spatial variance is indicative of increasing patchiness in the ecosystem, such as areas of high-  
178 density algal biomass and areas of low-density biomass within a lake. Spatial autocorrelation  
179 accounts for the location of those patches within the ecosystem in relationship to each other.  
180 Local Moran's I quantifies how similar the abundance of algae is at one location compared to the  
181 density of surrounding neighbors. When measured over time for variables that are indices of  
182 algal biomass (e.g., the pigments chlorophyll *a* and phycocyanin), both of these metrics of spatial  
183 heterogeneity can provide insight into the dynamics of algal bloom development. In models of

184 algal blooms, both spatial variance and autocorrelation are expected to be high during the bloom  
185 period (Buelo et al., 2018).

186 Spatial autocorrelation (AC) and the coefficient of variation (CV) were calculated for  
187 each variable on each sampling date in order to evaluate the dynamics of these parameters over  
188 time. Prior to analysis, extreme outliers in the algal pigments were removed from the spatial  
189 dataset as they were well outside the operating range of the Total Algae sensor or there was  
190 known interference with the sensor resulting in an inaccurate measurement. This resulted in five  
191 chlorophyll *a* and three phycocyanin measurements being removed out of 3,136 total pigment  
192 measurements. The spatial CV is the standard deviation of all of the spatial measurements for a  
193 variable on a given sampling date divided by the mean of those measurements, expressed as a  
194 percent. Spatial AC was calculated as the average value of local Moran's I with a queen's  
195 distance neighbor list (92 meters) with equal weight (1/n) on neighbors, as to not impose any  
196 assumptions on possible spatial patterns in the variables. We limited our analysis to surrounding  
197 neighbors because distances beyond this have not shown high spatial autocorrelation of algal  
198 pigments under experimental conditions (Butitta et al. 2017). Local Moran's I values near 1.0  
199 reflect high spatial AC within neighbors, zero indicates a random distribution, whereas spatial  
200 AC values nearing -1.0 indicate a perfectly dispersed distribution (e.g. checkerboard pattern) in  
201 the variable being measured. As the spatial variability in temperature is mediated by physical  
202 processes, we used the dynamics and extent of the spatial AC of temperature as a benchmark to  
203 visually compare the dynamics of spatial AC in the other biological variables. This allowed us to  
204 tease apart the effect of physically- versus biologically-driven spatial patterns. Additionally, in  
205 order to better visualize the spatial patterns in chlorophyll *a*, phycocyanin, temperature,

206 dissolved oxygen, and pH over the course of the season, the data were interpolated using inverse  
207 distance weighting across a 25m grid (Figure 2).

208 In order to evaluate if high frequency measurements at a fixed station are an adequate  
209 characterization of the surface water dynamics in a shallow lake, we compared the measurements  
210 taken by the fixed station sonde during the same time period as a spatial sampling event. High  
211 frequency data from the fixed station sonde was trimmed to the period that we sampled the lake  
212 spatially. A t-test with a Bonferroni correction, to account for the multiple comparisons, was  
213 performed to compare the distribution from the 98 sampling stations to the fixed station  
214 measurements from the same day for each of the four biologically-mediated variables,  
215 chlorophyll, phycocyanin, dissolved oxygen, and pH. In addition to comparing fixed sonde  
216 values to the spatial sampling, we also used the spatial data to identify locations in the lake that  
217 were consistently representative of mean conditions, and therefore ideal locations for fixed  
218 station monitoring. We identified locations in the lake for each sampling event that had  
219 measurements within the range of  $\pm$  one standard deviation from the mean for each biologically  
220 mediated variable (all variables except temperature). We then collated these locations across all  
221 sampling dates to identify which of the 98 sampling locations had measurements that most  
222 consistently represented the mean conditions of the lake.

223 Finally, we performed a rarefaction analysis to evaluate the optimal spatial sampling  
224 frequency to capture the mean value of the biologically-mediated variables. This was done by  
225 randomly selecting  $n$  number of spatial sampling data points ( $n=2-97$ ) during a sampling event,  
226 calculating the mean value from that subset, and then calculating the root mean square error  
227 (RMSE), comparing the mean estimate from the subset to the mean of all sampling points during  
228 that event. This calculation was repeated 1000 times for each value of  $n$ , and each iteration was

229 then averaged. The averaged RMSE values for each subset of  $n$  were fit using a local polynomial  
230 regression with a smoothing factor of 0.1 and each sampling event's RMSE curve was  
231 standardized by subtracting the mean of all iterations ("global mean") from the mean at  $n$   
232 number of stations, to aid in visual comparison. The spatial data are available through (Ortiz &  
233 Wilkinson, 2019) and the fixed station data are available in (Ortiz et al., 2019) and further  
234 analyzed in Ortiz et al. (2020). All analyses were performed using R 4.0.2 (R Core Team, 2020)  
235 using the gstat (Pebesma, 2004), rstatix (Kassambara, 2020), and sf packages (Pebesma, 2018).

236

## 237 **Results**

238         There were two bloom events during the summer of 2018 in Swan Lake. The first bloom  
239 occurred from DOY 156 – 184 and was dominated by the diatom *Aulacoseira spp.* based on a  
240 sample taken on DOY 177 examined under a compound microscope at 400x magnification. The  
241 phycocyanin concentrations on DOY 177 were the lowest during this first bloom period (Figure  
242 2), and no cyanobacteria were identified in the sample. The second bloom, peaking on DOY 236,  
243 was dominated by the cyanobacterium *Microcystis spp.* There were also two large precipitation  
244 events during the summer, occurring after sampling on DOY 170 and lasting through DOY 171,  
245 and on DOY 232 (Figure 2; Supplemental Figure 1). The maximum wind speed recorded during  
246 the first precipitation event was 10.8 m s<sup>-1</sup> coming from the southwest and 11.8 m s<sup>-1</sup> during the  
247 second precipitation event coming from the southeast. During the first half of the summer (DOY  
248 142 – 191) the prevailing winds 24 hours prior to the sampling events were from the south,  
249 switched to being predominantly from the north from DOY 198 – 219, and then varied in  
250 direction for the rest of the season (Figure 2). The median wind speed for the first period when  
251 winds were out of the south was 3.6 m s<sup>-1</sup> (Figure 3b). When the winds switched to being

252 predominantly from the north between DOY 198 – 219, the median wind speed was lower at 2.5  
253 m s<sup>-1</sup> (Figure S1).

#### 254 *Spatial dynamics*

255         During the two bloom periods there was not a latitudinal or longitudinal trend in  
256 chlorophyll *a* concentrations; instead, there were patches of high chlorophyll *a* concentration on  
257 otherwise low-concentration dates (Figure 2). Unlike chlorophyll *a*, phycocyanin had a strong  
258 latitudinal trend with higher concentrations in the northern portion (sample sites A1-G4) of the  
259 lake during the first bloom. This spatial pattern is readily observed on DOY 184 but is also  
260 noticeable for many of the sampling events during the first bloom (Figure 2). During sampling  
261 events with a strong latitudinal gradient in phycocyanin (DOY 166 – 184, and 236) the mean  
262 concentration in the northern portion of the lake was nearly double the concentration in the  
263 southern portion of the lake (7.29 and 3.76 µg L<sup>-1</sup>, respectively). On these dates, the prevailing  
264 winds 24 hours prior to the sampling event were out of the north (Supplemental Figure S1), yet  
265 the lowest concentrations of phycocyanin were found in the southern portion of the lake. Even  
266 when the lake was not blooming, there were patches of high concentrations of phycocyanin in  
267 the northern portion of the lake (e.g., DOY 212), located among the densest patch of American  
268 Lotus (Figure 1). The average phycocyanin concentrations at the sampling locations within the  
269 American Lotus patch was higher than the average concentration in the rest of the lake for 14 of  
270 the 16 sampling events (Figure S2).

271         The daytime saturation of dissolved oxygen varied the most out of the five variables  
272 monitored, ranging from borderline hypoxic (30% saturation) to supersaturated (up to 350%)  
273 (Figure 2). While the dissolved oxygen saturation increased near the peak of the bloom, the  
274 highest average saturation was on DOY 191, after the first bloom had collapsed. There was a

275 weak pattern over the course of the season of higher saturation in the northern portion of the  
276 lake, similar to the distribution of higher phycocyanin concentrations. However, within the  
277 northern portion of the lake, regions of low dissolved oxygen saturation formed in the surface  
278 waters, particularly later in the summer (Figure 1). Beginning on DOY 198, the mean dissolved  
279 oxygen concentration in the American lotus patch was consistently lower than the average for the  
280 rest of the lake until DOY 250 (Figure S2). The distribution of pH also had a weak spatial pattern  
281 during the summer, with slightly elevated values in the northern portion of the lake during the  
282 first bloom (e.g. DOY 177; Figure 2). While pH was elevated at the onset of the first bloom  
283 period from DOY 149 – 170, it was highest overall on DOY 191 and 198 after the first bloom  
284 had collapsed. Unlike the other variables, temperature had a subtle south to north latitudinal  
285 gradient with warmer temperatures in the southern portion of the lake and colder in the north  
286 during the latter half of the summer (Figure 2). On average this difference between the northern  
287 portion of the lake and the southern was 0.5°C. The warmest day of sampling was DOY 191.

288         Spatial variability in algal pigments during the first bloom event was low, with two  
289 exceptions. There was an increase in the CV of chlorophyll *a* on the last day of the bloom (DOY  
290 184; Figure 3a) that continued to increase as the bloom collapsed. There was also a temporary  
291 increase in phycocyanin CV during the first bloom on DOY 177 (Figure 3b), coinciding with a  
292 temporary decline in phycocyanin concentration across the lake. The CV of both algal pigments  
293 was higher than the CV of temperature over the course of the entire sampling period.

294         Conversely, the CV of pH and dissolved oxygen were elevated during the first bloom  
295 period, with pH CV declining and remaining low after the first bloom (Figure 3c) and dissolved  
296 oxygen CV only temporarily declining after the first bloom (Figure 3d). Temperature had low  
297 variability throughout the first bloom until DOY 177, when the lake began to heat up, peaking in

298 both temperature and spatial variability on DOY 191 (Figure 3e). Between the first and second  
299 bloom, DOY 191-226, there was a decrease in spatial variability among the algal pigments and  
300 pH as the bloom collapsed, while temperature and dissolved oxygen CV remained relatively high  
301 and variable. During the second bloom period, CV was low for all variables except for  
302 chlorophyll *a*. In general, the CV, of temperature and pH, expressed as a percentage, was an  
303 order of magnitude lower than the other variables.

304         Spatial autocorrelation (AC), quantified as local Moran's I, did not fall substantially  
305 below 0 for any of the variables and peaked at 0.79 among all variables (Figure 3). The highest  
306 AC value for chlorophyll *a* and phycocyanin was during the first bloom event (Figure 3f, g);  
307 however, phycocyanin AC also increased substantially during the second bloom. During the first  
308 bloom, the AC of temperature varied similarly to both pigments' AC, particularly phycocyanin,  
309 but became decoupled after the bloom collapsed. While the AC of temperature remained high  
310 during the inter-bloom period, the AC of the pigments was substantially lower. Conversely, the  
311 dynamics of AC of temperature, dissolved oxygen and pH remained coupled throughout the  
312 summer (Figure 3h, i). Dissolved oxygen saturation and pH both increased in AC during the first  
313 bloom and then declined throughout the rest of the season with the exception of a minor increase  
314 in AC during the second bloom event.

315

#### 316 *Fixed station versus spatial sampling*

317         There were a greater number of days with a significant difference between the spatial and  
318 fixed station measurements than days in which the data sets were not significantly different  
319 (Figure 4). Among all 64 comparisons (4 variables  $\times$  16 sampling events), the spatial and fixed  
320 station data sets had a means that were not significantly different 37.5% of the time.

321 Phycocyanin had the greatest number of events with similar values, with 7 of the 16 sampling  
322 events having non-statistically different mean values measured spatially and at the fixed station  
323 (Figure 4b). These occurrences were mainly during non-bloom periods. However, even when the  
324 mean phycocyanin values were similar between the sampling methods on a given day, the range  
325 of values captured by the fixed station was five times less than the variability captured in the  
326 spatial data. This pattern of infrequent occurrences of similar mean values between the two  
327 methods during non-bloom periods and a diminished range in the fixed station data, was shared  
328 to a degree, among the other three variables as well. Interestingly, dissolved oxygen saturation  
329 only had 5 out of the 16 events with means that were not significantly different, all of which  
330 occurred when the lake was above 100% saturation (Figure 4c).

331 While a majority of the comparisons between the fixed station and spatial data indicate  
332 that the algal pigments had a larger range of values in the spatial data, there were a handful of  
333 instances where the opposite was true. During the first bloom, the fixed station sonde measured a  
334 wide range of chlorophyll *a* concentrations and had a higher mean chlorophyll *a* for all dates  
335 (Figure 4a). Similarly, we observed higher mean phycocyanin at the fixed station sonde on DOY  
336 156, 166, 177, 191, and 219 (Figure 4b). However, this pattern did not hold true for dissolved  
337 oxygen or pH (Figure 5c, d).

338 The spatial sampling sites that most consistently captured the mean values in the lake on  
339 a given sampling date were in the northwest portion of the lake, near the inlet. The best  
340 performing site for all variables was site E3, just west of the American lotus patch and adjacent  
341 to a bed of sago pondweed (Figure 1). The four biologically-mediated variables from sample site  
342 E3 were within the mean ( $\pm$  standard deviation) range of all of the spatial measurements 95% of  
343 the time. The second best performing location was in the middle of the American lotus patch, site



344 D4, with the values from this site being within the mean ( $\pm$  standard deviation) range 92% of the  
345 time. The site where the fixed station was located, site H2, was only within the mean ( $\pm$  standard  
346 deviation) range 58% of the time.

347

### 348 *Optimal Spatial Resolution*

349 In order to evaluate the spatial sampling resolution needed to capture the mean state of  
350 the surface water on a given day, we performed a rarefaction analysis for each variable and each  
351 sampling event, calculating the root mean squared error (RMSE) of a subset of sampling  
352 locations compared to the mean value of all 98 measurements that day. The plateaus of the  
353 RMSE curves from the rarefaction analysis were used to evaluate the smallest number of spatial  
354 sampling locations needed to capture the mean across the lake during that sampling event (Figure  
355 5). Additionally, we also evaluated the temporal pattern of the minimum number of sampling  
356 locations needed to capture the mean.

357 Mean values were underestimated for all variables on all sampling dates when there were  
358 less than 10 sampling stations (Figure 5). However, the severity of the underestimation differed  
359 among the variables. The rarefaction analysis for chlorophyll *a* indicated that 10 – 30 sampling  
360 locations was sufficient for capturing the mean chlorophyll *a* in Swan Lake, otherwise the mean  
361 concentration would be under estimated (Figure 5a). When an algal bloom was occurring it took  
362 more sampling locations to near the mean chlorophyll *a* concentration on that date. However,  
363 when the bloom was particularly patchy during development (DOY 226) or collapse (DOY 191),  
364 including a larger number of sampling locations led to overestimating the mean chlorophyll *a*  
365 concentration as locations with high concentrations were over-represented in the data set. There  
366 were similar patterns in phycocyanin RMSE with most sampling dates plateauing between 20 –

367 30 sampling locations with a few exceptions (Figure 5b). For DOYs 156-170 (rise of the first  
368 bloom) and 212, at least 60 sampling locations were needed to capture the overall mean in  
369 phycocyanin for that sampling date. Dissolved oxygen saturation and pH were generally well  
370 characterized by approximately 10 – 15 sampling locations as both had a majority of dates in  
371 which the RMSE curves plateaued at that spatial sampling resolution (Figure 5c, d). However, at  
372 the beginning (DOY 154), peak (DOY 184), and end (DOY 205) of the first bloom, twice as  
373 many sampling locations were needed to capture the mean dissolved oxygen. Only two dates  
374 required more sampling locations for pH to capture the mean, DOY 177 and 198, which  
375 plateaued at approximately 40 sampling locations. The largest RMSE were observed during  
376 bloom conditions for all variables: DOY 177 had the largest error for phycocyanin and pH, while  
377 the largest RMSE was on DOY 184 for dissolved oxygen and on DOY 236 for chlorophyll *a*  
378 (Figure 5).

379

## 380 **Discussion**

381 The spatial heterogeneity of water quality parameters was highly dynamic in Swan Lake,  
382 a shallow, hypereutrophic, temperate waterbody. The temporal dynamics in heterogeneity were  
383 driven in part by the two blooms, the peaks of which were preceded by large precipitation events.  
384 These rain events could have delivered nutrients from the agriculturally dominated watershed  
385 into the lake from the northern inlet, helping to fuel the subsequent algal blooms and the spatial  
386 patterns observed during blooms (Stockwell et al. 2020). However, there are also a number of  
387 other factors that likely contributed to the spatial variability and pattern during and following  
388 these bloom events, including the prevailing wind direction prior to sampling, the bathymetry of

389 the basin and location of the surface inlet, and the potential for dense macrophyte beds to  
390 contribute to local patchiness.

391 The spatial patterns that the algal blooms created were consistent with the expectations  
392 from previous modeling and experimental work that spatial AC increases as algal blooms  
393 develop (Buelo et al., 2018; Butitta et al., 2017; Serizawa et al., 2008). This pattern was the  
394 strongest for phycocyanin, evident by the strong latitudinal gradient in concentrations during the  
395 bloom periods. The sampling dates with phycocyanin concentration gradients (e.g., DOY 166,  
396 177, 184, 236) coincided with persistent winds from the south 24 hours prior to the sampling  
397 event, which likely resulted in the higher concentration of algal cells in the northern portion of  
398 the lake. The effect of persistent wind directions influencing the distribution of cyanobacteria has  
399 also been documented in other shallow eutrophic lakes (Wu et al. 2010). The shallow sediments  
400 of the northern basin were also likely a source of akinete recruitment (Karlsson-Elfgren and  
401 Brunburg, 2004), further contributing to the higher concentrations of phycocyanin in the northern  
402 portion of the lake during the first bloom. Augmented nutrient availability in the northern part of  
403 the lake due to external loading from the watershed through the surface inlet and internal loading  
404 from the sediments overlain by an unstratified water column (Song and Burgin 2017) may have  
405 further amplified the phytoplankton gradient, particularly following precipitation events. Finally,  
406 the tendency of the dominant cyanobacteria taxa *Microcystis spp.* to form surface scums likely  
407 enhanced the spatial patterns observed with our surface sampling approach.

408 The sampling dates with a strong gradient of phytoplankton concentrations from north to  
409 south also resulted in north-south gradients in water chemistry. On these dates, both dissolved  
410 oxygen and pH formed a gradient of high values in the northern portion of the lake and lower  
411 values in the south, which would be expected with greater primary production where

412 phytoplankton concentrations were highest. The spatial patterns in the surface water chemistry  
413 demonstrate how phytoplankton spatial distribution, driven by wind, can create hot spots and  
414 moments of biogeochemical activity within lakes (McClain et al. 2003) that may be missed with  
415 traditional, single-station sampling. The dense patch of floating leaf American lotus macrophytes  
416 also created a hot spot of biogeochemical activity.

417         Macrophyte beds can have a large local influence on water chemistry by inducing  
418 stratification, decreasing flow and trapping particles, and modifying the light environment  
419 (Green, 2006; Vilas et al., 2017). For 87.5% of the season the phycocyanin concentrations were  
420 higher in the bed of American lotus than concentrations elsewhere in the lake. In fact, even on  
421 sampling dates when phycocyanin concentrations were otherwise low (e.g., DOY 212), the  
422 American lotus patch can be identified based on the phycocyanin concentrations that are nearly  
423 twice as high as the rest of the lake. We hypothesize that the macrophyte patch allowed for  
424 microstratification in the water column and reduced wind-driven flow. These physical conditions  
425 are likely to favor cyanobacteria dominance and the formation of surface scums. Similarly, the  
426 dissolved oxygen concentrations in the American lotus patch became consistently lower than the  
427 rest of the lake later in the summer, likely due to the plants beginning to senesce, creating a hot  
428 spot of decomposition, decreasing both dissolved oxygen and pH (Vilas et al., 2017). While there  
429 isn't strong evidence in the data that the other submerged macrophyte beds had a similarly strong  
430 effect on water chemistry, the data from the American lotus patch illustrates how macrophytes  
431 can contribute to local patchiness and overall spatial heterogeneity.

432

433 *Considerations for Monitoring*

434           The variables that we measured in this study are often the target of water quality  
435 monitoring as the dynamics of these variables coincide with changes in ecosystem function and  
436 services. Monitoring is often performed at a fixed station over time to capture the dynamics of  
437 the ecosystem, but this strategy could potentially result in missed information about the  
438 ecosystem's behavior. While the temporal dynamics of all the variables were synchronous  
439 between the fixed station and spatial sampling data sets in Swan Lake, our conclusions regarding  
440 the magnitude of the blooms and variability in the lake's structure would have been substantially  
441 different relying solely on the fixed station data. Among the four biologically-mediated  
442 variables, only 37.5% of the fixed station estimates of the mean state of the lake statistically  
443 matched the estimate from the spatial sampling. The vast majority of those instances (96%)  
444 occurred during non-bloom periods, which also coincided with lower wind speed conditions, no  
445 prevailing wind direction, and no major precipitation events. The large difference between the  
446 spatial sampling and fixed station measurements of algal pigments during blooms was likely  
447 driven, in part, by the depth of the sensors at the fixed station and the variable accumulation of  
448 cyanobacteria at the surface of the lake dependent upon environmental conditions and the  
449 dominant taxa (Chaffin et al., 2020). It is clear from our data that during periods of heightened  
450 biological activity such as blooms, fixed station monitoring is unlikely to be representative of the  
451 mean ecosystem state in shallow lakes.

452           Despite the high degree of horizontal spatial variability that has been documented in this  
453 study and others (Loken et al. 2019, Van de Bogert et al. 2012, Buttita et al. 2017), fixed station  
454 designs are widely used in water quality monitoring programs. In Swan Lake, we determined that  
455 the historical location for water quality monitoring, where the fixed station sensors were  
456 deployed, was one of the least-representative locations for mean conditions in the lake. Given the

457 hypereutrophic state of the lake, the most immediate management concerns are toxic  
458 cyanobacteria blooms and summer fish kills due to low dissolved oxygen. Yet, the mean value of  
459 these variables (phycocyanin and dissolved oxygen) across the lake were only captured by the  
460 fixed station sensors 58% of the time. While selecting a fixed station site for high frequency  
461 sensor deployment includes many considerations including the location of previous data  
462 collection and management needs, based on our analysis we would advise performing a spatial  
463 survey to identify if and when the fixed station site is representative of mean conditions in the  
464 lake. A complementary spatial survey will help contextualize the fixed station dynamics and  
465 provide additional, management-relevant information about the lake.

466         It's also important to consider the trade-offs between high frequency fixed station  
467 monitoring and higher resolution, but less frequent spatial monitoring. High frequency  
468 monitoring at a single station provides insight into ecosystem function such as metabolism  
469 (Staeher et al., 2012), early warnings of impending regime shifts (Carpenter et al., 2011;  
470 Wilkinson et al., 2018), and crucial information on diel variability in limnological conditions  
471 (Andersen et al., 2017). However, as we observed in Swan Lake, the spatial variability within a  
472 given day often exceeds the temporal variability at a single point in a shallow lake. Without the  
473 spatial sampling snapshots, we would have underestimated the magnitude of the algal blooms,  
474 hampering our limnological understanding of the ecosystem's functioning and impeding our  
475 ability to accurately estimate rates such as methane emissions on a global scale (DelSontro et al.  
476 2018).

477         From a practical stand point, the understanding gleaned from the spatial sampling could  
478 help managers design targeted algal toxin monitoring or management interventions to help  
479 control fish habitat quality in persistently hypoxic areas (Bardshaw et al., 2015). However, the

480 time and cost investment in repeated spatial sampling at the resolution performed in this study  
481 may not be feasible for both research and management programs. The rarefaction analysis we  
482 performed for all four of the key water quality monitoring variables revealed that minimal  
483 information was gained after ~30 locations were sampled across many conditions and variables.  
484 Often 12-20 sample locations across the 40.5 ha lake (or a 1-2 samples per hectare) was  
485 sufficient to capture the spatial variability within the lake, with a few exceptions. These  
486 exceptions occurred during times of higher variability such as when the blooms were just starting  
487 or when the bloom began to collapse. The need for a higher spatial resolution during bloom  
488 events to fully capture their variability has also been found using remote sensing techniques in  
489 other, larger lakes (Lekki et al., 2019). As the spatial resolution of remote sensing technologies  
490 continues to improve, it may become more cost effective to capture the spatial heterogeneity of  
491 algal pigments in small lakes over time. However, one of the benefits of manual spatial sampling  
492 is being able to pair other measurements such as dissolved oxygen, pH, and nutrients (e.g.,  
493 nitrate; Loken et al., 2018; Pellerin et al., 2016) with information on the distribution of algal  
494 biomass.

495         Our intensive spatial monitoring of a shallow, hypereutrophic lake revealed how spatially  
496 heterogeneous shallow lakes are over the course of a single season and allowed us to tease apart  
497 the drivers of that spatial heterogeneity. We found that variability was greatest during  
498 biologically-intensive periods, such as during algal blooms and in dense floating-leaf macrophyte  
499 beds, and that failure to capture this variability would have hampered our understanding of the  
500 ecosystem's functioning and overall mean state. Small lakes such as Swan Lake dominate the  
501 global distribution of waterbodies (Verpoorter et al. 2014). Adequately capturing and  
502 characterizing the magnitude of variability in production of these waterbodies is important given

503 their role in mediating global nutrient cycles (Downing et al. 2010, Biddanda et al. 2017),  
504 especially methane emissions (DelSontro et al. 2018, Loken et al. 2019). Our data provided an  
505 estimate of the spatial resolution needed to capture the dynamics in ecosystems similar to Swan  
506 Lake and a method which could be readily adapted to other ecosystems. While our results  
507 provide new understanding of the magnitude and temporal dynamics of spatial heterogeneity in  
508 shallow lakes, continued investigation of horizontal spatial heterogeneity in a range of aquatic  
509 ecosystems, from oligotrophic to eutrophic, is needed to better understand the structure and  
510 drivers of horizontal spatial variability in lakes.

511

## 512 **Acknowledgments**

513 We would like to thank Ryan Wagner, Ellen Albright, Rachel Fleck and Tyler Butts for  
514 assistance with data collection and instrument deployment and collection. We would also like to  
515 thank two anonymous reviewers and the editor for constructive comments that improved the  
516 manuscript. Funding was provided by the Center for Global and Regional Environmental  
517 Research, the Iowa State University Graduate Minority Assistantship Program, and the Iowa  
518 State University Graduate Research Assistantship Match Program.

519

## 520 **References**

- 521 American Public Health Association (APHA), American Water Works Association (AWWA),  
522 and the Water Environmental Federation (WEF). 1998. Standard Methods for  
523 Examinations of Water and Wastewater, 20th ed. United Book Press, Inc. Baltimore,  
524 Maryland.
- 525 Andersen, M. R., Kragh, T., & Sand-Jensen, K. (2017). Extreme diel dissolved oxygen and  
526 carbon cycles in shallow vegetated lakes. *Proceedings of the Royal Society B-Biological*  
527 *Sciences*, 284(1862), doi:10.1098/rspb.2017.1427
- 528 Angradi, T. R., Ringold, P. L., & Hall, K. (2018). Water clarity measures as indicators of  
529 recreational benefits provided by US lakes: Swimming and aesthetics. *Ecological*  
530 *Indicators*, 93, 1005-1019. doi:10.1016/j.ecolind.2018.06.001



- 531 Bardshaw, E. L., Allen, M. S., & Netherland, M. (2015). Spatial and temporal occurrence of  
532 hypoxia influences fish habitat quality in dense *Hydrilla verticillata*. *Journal of*  
533 *Freshwater Ecology*, 30(4), 491-502.
- 534 Biddanda, B. A. (2017). Global significance of the changing freshwater carbon cycle. *EOS*, 98,  
535 doi:10.1029/2017EO069751
- 536 Boehrer, B., & Schultze, M. (2008). Stratification of lakes. *Reviews of Geophysics*, 46(2),  
537 doi:10.1029/2006rg000210
- 538 Buelo, C. D., Carpenter, S. R., & Pace, M. L. (2018). A modeling analysis of spatial statistical  
539 indicators of thresholds for algal blooms. *Limnology and Oceanography Letters*, 3(5),  
540 384-392. doi:10.1002/lol2.10091
- 541 Butitta, V. L., Carpenter, S. R., Loken, L. C., Pace, M. L., & Stanley, E. H. (2017). Spatial early  
542 warning signals in a lake manipulation. *Ecosphere*, 8(10), doi:10.1002/ecs2.1941
- 543 Carlson, R. E. (1977). Trophic State Index for Lakes. *Limnology and Oceanography*, 22(2), 361-  
544 369. doi:10.4319/lo.1977.22.2.0361
- 545 Carpenter, S., Booth, E., Kucharik, C., & Lathrop, R. (2015). Extreme daily loads: role in annual  
546 phosphorus input to a north temperate lake. *Aquatic Sciences*, 77(1), 71-79.  
547 doi:10.1007/s00027-014-0364-5
- 548 Carpenter, S. R., Arani, B. M. S., Hanson, P. C., Scheffer, M., Stanley, E. H., & Van Nes, E.  
549 (2020). Stochastic dynamics of Cyanobacteria in long-term high-frequency observations  
550 of a eutrophic lake. *Limnology and Oceanography Letters*, 5(5), 331-336.  
551 doi:10.1002/lol2.10152
- 552 Carpenter, S. R., Cole, J. J., Pace, M. L., Batt, R., Brock, W. A., Cline, T., . . . Weidel, B. (2011).  
553 Early Warnings of Regime Shifts: A Whole-Ecosystem Experiment. *Science*, 332(6033),  
554 1079-1082. doi:10.1126/science.1203672
- 555 Chaffin, J. D., Kane, D. D., & Johnson, A. (2020). Effectiveness of a fixed-depth sensor  
556 deployed from a buoy to estimate water-column cyanobacterial biomass depends on wind  
557 speed. *Journal of Environmental Sciences*, 93, 23-29, doi:10.1016/j.jes.2020.03.003
- 558 Christensen, J. P. A., Sand-Jensen, K., & Staehr, P. A. (2013). Fluctuating water levels control  
559 water chemistry and metabolism of a charophyte-dominated pond. *Freshwater Biology*,  
560 58(7), 1353-1365. doi:10.1111/fwb.12132
- 561 Codd, G. A., Morrison, L. F., & Metcalf, J. S. (2005). Cyanobacterial toxins: risk management  
562 for health protection. *Toxicology and Applied Pharmacology*, 203(3), 264-272.  
563 doi:10.1016/j.taap.2004.02.016
- 564 Corbel, S., Mougin, C., & Bouaicha, N. (2014). Cyanobacterial toxins: Modes of actions, fate in  
565 aquatic and soil ecosystems, phytotoxicity and bioaccumulation in agricultural crops.  
566 *Chemosphere*, 96, 1-15. doi:10.1016/j.chemosphere.2013.07.056
- 567 Cotterill, V., Hamilton, D. P., Puddick, J., Suren, A., & Wood, S. A. (2019). Phycocyanin  
568 sensors as an early warning system for cyanobacteria blooms concentrations: a case study  
569 in the Rotorua lakes. *New Zealand Journal of Marine and Freshwater Research*, 53(4),  
570 555-570. doi:10.1080/00288330.2019.1617322
- 571 Davis, T. W., Berry, D. L., Boyer, G. L., & Gobler, C. J. (2009). The effects of temperature and  
572 nutrients on the growth and dynamics of toxic and non-toxic strains of *Microcystis* during  
573 cyanobacteria blooms. *Harmful Algae*, 8(5), 715-725. doi:10.1016/j.hal.2009.02.004
- 574 DelSontro, T., Beaulieu, J. J., & Downing, J. A. (2018). Greenhouse gas emissions from lakes  
575 and impoundments: Upscaling in the face of global change. *Limnology and*  
576 *Oceanography Letters*, 3(3), 64-75. doi:10.1002/lol2.10073

577 Dodds, W. K., Bouska, W. W., Eitzmann, J. L., Pilger, T. J., Pitts, K. L., Riley, A. J., . . .  
578 Thornbrugh, D. J. (2009). Eutrophication of US Freshwaters: Analysis of Potential  
579 Economic Damages. *Environmental Science & Technology*, 43(1), 12-19.  
580 doi:10.1021/es801217q

581 Downing, J. A. 2010. Emerging global role of small lakes and ponds: little things mean a lot.  
582 *Limnetica* 29(1), 9-24.

583 George, D. G., & Heaney, S. I. (1978). Factors influencing spatial-distribution of phytoplankton  
584 in a small productive lake. *Journal of Ecology*, 66(1), 133-155. doi:10.2307/2259185

585 Gilbert, P. M. (2017). Eutrophication, harmful algae and biodiversity - Challenging paradigms in  
586 a world of complex nutrient changes. *Marine Pollution Bulletin*, 124(2), 591-606.  
587 doi:10.1016/j.marpolbul.2017.04.027

588 Green, J. C. (2006). Effect of macrophyte spatial variability on channel resistance. *Advances in*  
589 *Water Resources*, 29(3), 426-438. doi:10.1016/j.advwatres.2005.05.010

590 Hansen, A. M., Andersen, F. O., & Jensen, H. S. (1997). Seasonal pattern in nutrient limitation  
591 and grazing control of the phytoplankton community in a non-stratified lake. *Freshwater*  
592 *Biology*, 37(3), 523-534. doi:10.1046/j.1365-2427.1997.00182.x

593 Kassambara, A. (2020). rstatix: Pipe-Friendly Framework for Basic Statistical Tests. R package  
594 version 0.6.0. Retrieved from <https://cran.r-project.org/package=rstatix>

595 Karlsson-Elfgren, I., & Brunberg, A. K. (2004). The importance of shallow sediments in the  
596 recruitment of Anabaena and Aphanizomenon (Cyanophyceae). *Journal of Phycology*,  
597 40(5), 831-836. doi:10.1111/j.1529-8817.2004.04070.x

598 Kelly, P. T., Renwick, W. H., Knoll, L., & Vanni, M. J. (2019). Stream Nitrogen and Phosphorus  
599 Loads Are Differentially Affected by Storm Events and the Difference May Be  
600 Exacerbated by Conservation Tillage. *Environmental Science & Technology*, 53(10),  
601 5613-5621. doi:10.1021/acs.est.8b05152

602 Laas, A., Noges, P., Koiv, T., & Noges, T. (2012). High-frequency metabolism study in a large  
603 and shallow temperate lake reveals seasonal switching between net autotrophy and net  
604 heterotrophy. *Hydrobiologia*, 694(1), 57-74. doi:10.1007/s10750-012-1131-z

605 Landsberg, J. H. (2002). The effects of harmful algal blooms on aquatic organisms. *Reviews in*  
606 *Fisheries Science*, 10(2), 113-390. doi:10.1080/20026491051695

607 Lekki, J., Deutsch, E., Sayers, M., Bosse, K., Anderson, R., Tokars, R., & Sawtell, R. (2019).  
608 Determining remote sensing spatial resolution requirements for the monitoring of harmful  
609 algal blooms in the Great Lakes. *Journal of Great Lakes Research*, 45(3), 434-443.  
610 doi:10.1016/j.jglr.2019.03.014

611 Loken, L. C., Crawford, J. T., Dornblaser, M. M., Striegl, R. G., Houser, J. N., Turner, P. A., &  
612 Stanley, E. H. (2018). Limited nitrate retention capacity in the Upper Mississippi River.  
613 *Environmental Research Letters*, 13(7). doi:10.1088/1748-9326/aacd51

614 Loken, L. C., Crawford, J. T., Schramm, P. J., Stadler, P., Desai, A. R. & Stanley, E. H. (2019).  
615 Large Spatial and Temporal Variability of Carbon Dioxide and Methane in a Eutrophic  
616 Lake. *Journal of Geophysical Research-Biogeosciences*, 124(7), 2248-2266.  
617 10.1029/2019jg005186

618 McClain, M. E., Boyer, E. W., Dent, C. L., Gergel, S. E., Grimm, N. B., Groffman, P. M., ...  
619 Pinay, G. (2003). Biogeochemical hot spots and hot moments at the interface of terrestrial  
620 and aquatic ecosystems. *Ecosystems*, 6(4), 301-312. doi:10.1007/s10021-003-0161-9

621 Medeiros, A. S., Biastoch, R. G., Luszczek, C. E., Wang, X. A., Muir, D. C. G., & Quinlan, R.  
622 (2012). Patterns in the limnology of lakes and ponds across multiple local and regional

623 environmental gradients in the eastern Canadian Arctic. *Inland Waters*, 2(2), 59-76.  
624 doi:10.5268/iw-2.2.427

625 Moller, T. R., & Rordam, C. P. (1985). Species numbers of vascular plants in relation to area,  
626 isolation and age of ponds in Denmark. *Oikos*, 45(1), 8-16. doi:10.2307/3565216

627 Moran, P. A. P. (1950). Notes on Continuous Stochastic Phenomena. *Biometrika*, 37(1-2), 17-23.  
628 doi:10.2307/2332142

629 Moreno-Ostos, E., Cruz-Pizarro, L., Basanta, A., & George, D. G. (2009). Spatial Heterogeneity  
630 of Cyanobacteria and Diatoms in a Thermally Stratified Canyon-Shaped Reservoir.  
631 *International Review of Hydrobiology*, 94(3), 245-257. doi:10.1002/iroh.200811123

632 Ortiz, D., Palmer, J., & Wilkinson, G. (2019). Hypereutrophic lake sensor data during summer  
633 algae blooms in Iowa, USA, 2014 - 2018 ver 1. *Environmental Data Initiative*.  
634 doi:10.6073/pasta/30070d41fbcdf36387f33d9108f570f8

635 Ortiz, D., & Wilkinson, G. (2019). Hypereutrophic lake spatial sensor data during summer  
636 bloom, Swan Lake, Iowa, USA 2018 ver 1. *Environmental Data Initiative*.  
637 doi:10.6073/pasta/2c0ca177438a3d422925811514e86cd8

638 Ortiz, D., Palmer, J., & Wilkinson, G. (2020). Detecting changes in statistical indicators of  
639 resilience prior to algal blooms in shallow eutrophic lakes. *Ecosphere*, 11(10).  
640 doi:10.1002/ecs2.3200

641 Pace, M. L., Batt, R. D., Buelo, C. D., Carpenter, S. R., Cole, J. J., Kurtzweil, J. T., & Wilkinson,  
642 G. M. (2017). Reversal of a cyanobacterial bloom in response to early warnings.  
643 *Proceedings of the National Academy of Sciences of the United States of America*,  
644 114(2), 352-357. doi:10.1073/pnas.1612424114

645 Pebesma, E. J. (2018). Simple Features for R: Standardized Support for Spatial Vector Data. *R*  
646 *Journal*, 10(1), 439-446.

647 Pebesma, E. J. (2004). Multivariable geostatistics in S: the gstat package. *Computers &*  
648 *Geosciences*, 30(7), 683-691. doi:10.1016/j.cageo.2004.03.012

649 Pellerin, B. A., Stauffer, B. A., Young, D. A., Sullivan, D. J., Bricker, S. B., Walbridge, M. R.,  
650 ... Shaw, D. M. (2016). Emerging tools for continuous nutrient monitoring networks:  
651 sensors advancing science and water resources protection. *Journal of the American Water*  
652 *Resources Association*, 52(4), 993-1008. doi:10.1111/1752-1688.12386

653 R Core Team. (2020). R: A language and environment for statistical computing. R Foundation  
654 for Statistical Computing, Vienna, Austria. Retrieved from <https://www.R-project.org/>

655 Read, J. S., Hamilton, D. P., Jones, I. D., Muraoka, K., Winslow, L. A., Kroiss, R., ... Gaiser, E.  
656 (2011). Derivation of lake mixing and stratification indices from high-resolution lake  
657 buoy data. *Environmental Modelling & Software*, 26(11), 1325-1336.  
658 doi:10.1016/j.envsoft.2011.05.006

659 Rennella, A. M., & Quiros, R. (2006). The effects of hydrology on plankton biomass in shallow  
660 lakes of the Pampa Plain. *Hydrobiologia*, 556, 181-191. doi:10.1007/s10750-005-0318-y

661 Romo, S., Soria, J., Fernandez, F., Ouahid, Y., & Baron-Sola, A. (2013). Water residence time  
662 and the dynamics of toxic cyanobacteria. *Freshwater Biology*, 58(3), 513-522.  
663 doi:10.1111/j.1365-2427.2012.02734.x

664 Rychtecky, P., & Znachor, P. (2011). Spatial heterogeneity and seasonal succession of  
665 phytoplankton along the longitudinal gradient in a eutrophic reservoir. *Hydrobiologia*,  
666 663(1), 175-186. doi:10.1007/s10750-010-0571-6

667 Schilder, J., Bastviken, D., van Hardenbroek, M., Kankaala, P., Rinta, P., Stotter, T., & Heiri, O.  
668 (2013). Spatial heterogeneity and lake morphology affect diffusive greenhouse gas

669 emission estimates of lakes. *Geophysical Research Letters*, 40(21), 5752-5756.  
670 doi:10.1002/2013gl057669

671 Schoen, J. H., Stretch, D. D., & Tirok, K. (2014). Wind-driven circulation patterns in a shallow  
672 estuarine lake: St Lucia, South Africa. *Estuarine Coastal and Shelf Science*, 146, 49-59.  
673 doi:10.1016/j.ecss.2014.05.007

674 Serizawa, H., Amemiya, T., & Itoh, K. (2008). Patchiness in a minimal nutrient - phytoplankton  
675 model. *Journal of Biosciences*, 33(3), 391-403. doi:10.1007/s12038-008-0059-y

676 Smith, C., D. (2018). *Temporal and Spatial Monitoring of Cyanobacterial Blooms at Willow*  
677 *Creek Reservoir, North-Central Oregon*. Retrieved from U.S. Geological Survey  
678 Scientific Investigations Report:

679 Solomon, C. T., Bruesewitz, D. A., Richardson, D. C., Rose, K. C., Van de Bogert, M. C.,  
680 Hanson, P. C., . . . Zhu, G. W. (2013). Ecosystem respiration: Drivers of daily variability  
681 and background respiration in lakes around the globe. *Limnology and Oceanography*,  
682 58(3), 849-866. doi:10.4319/lo.2013.58.3.0849

683 Song, K., & Burgin, A. J. (2017). Perpetual Phosphorus Cycling: Eutrophication Amplifies  
684 Biological Control on Internal Phosphorus Loading in Agricultural Reservoirs.  
685 *Ecosystems*, 20(8), 1483-1493. doi:10.1007/s10021-017-0126-z

686 Staehr, P. A., Christensen, J. P. A., Batt, R. D., & Read, J. S. (2012). Ecosystem metabolism in a  
687 stratified lake. *Limnology and Oceanography*, 57(5), 1317-1330.  
688 doi:10.4319/lo.2012.57.5.1317

689 Stanley, E. H., Collins, S. M., Lottig, N. R., Oliver, S. K., Webster, K. E., Cheruvilil, K. S., &  
690 Soranno, P. A. (2019). Biases in lake water quality sampling and implications for  
691 macroscale research. *Limnology and Oceanography*, 64(4), 1572-1585.  
692 doi:10.1002/lno.11136

693 Stockwell, J. D., Doubek, J. P., Adrian, R., Anneville, O., Carey, C. C., Carvalho, L., . . . Wilson,  
694 H. L. (2020). Storm impacts on phytoplankton community dynamics in lakes. *Global*  
695 *Change Biology*, 26(5), 2756-2784. doi:10.1111/gcb.15033

696 United States Environmental Protection Agency. (1993a). *Determination of Nitrate-Nitrite by*  
697 *Automated Colorimetry. Method 353.2 Revision 2.0.*

698 United States Environmental Protection Agency. (1993b). *Determination of Phosphorus by*  
699 *Semi-Automated Colorimetry. Method 365.1 Revision 2.0.*

700 United States Environmental Protection Agency. (1993c). *Determination of Total Kjeldahl*  
701 *Nitrogen by Semi-Automated Colorimetry Method 351.2, Revision 2.0.*

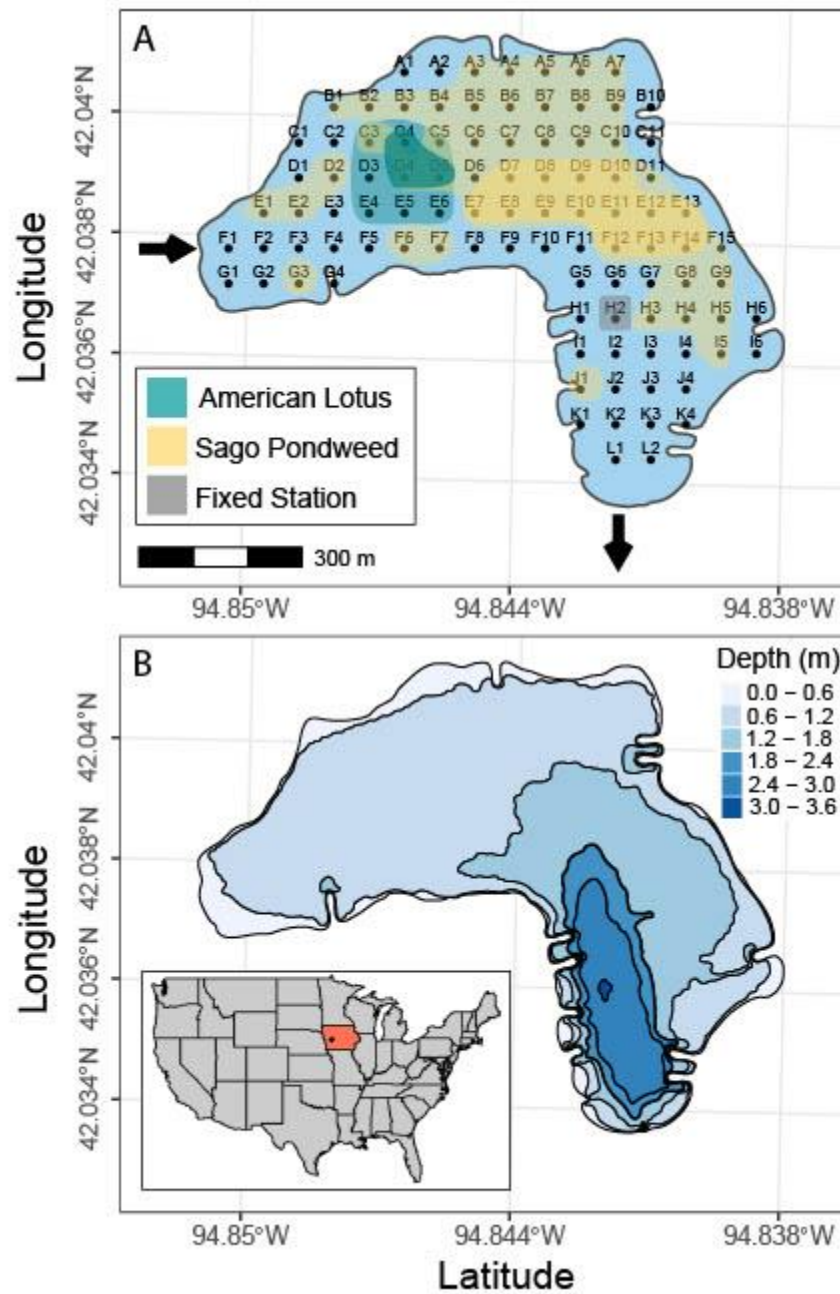
702 Van de Bogert, M. C., Bade, D. L., Carpenter, S. R., Cole, J. J., Pace, M. L., Hanson, P. C., &  
703 Langman, O. C. (2012). Spatial heterogeneity strongly affects estimates of ecosystem  
704 metabolism in two north temperate lakes. *Limnology and Oceanography*, 57(6), 1689-  
705 1700. doi:10.4319/lo.2012.57.6.1689

706 Vilas, M. P., Marti, C. L., Adams, M. P., Oldham, C. E., & Hipsey, M. R. (2017). Invasive  
707 Macrophytes Control the Spatial and Temporal Patterns of Temperature and Dissolved  
708 Oxygen in a Shallow Lake: A Proposed Feedback Mechanism of Macrophyte Loss.  
709 *Frontiers in Plant Science*, 8. doi:10.3389/fpls.2017.02097

710 Verpoorter, C., Kutser, T., Seekell, D. A., & Tranvik, L. J. (2014). A global inventory of lakes  
711 based on high-resolution satellite imagery. *Geophysical Research Letters*, 41(18), 6396-  
712 6402. doi:10.1002/2014gl060641

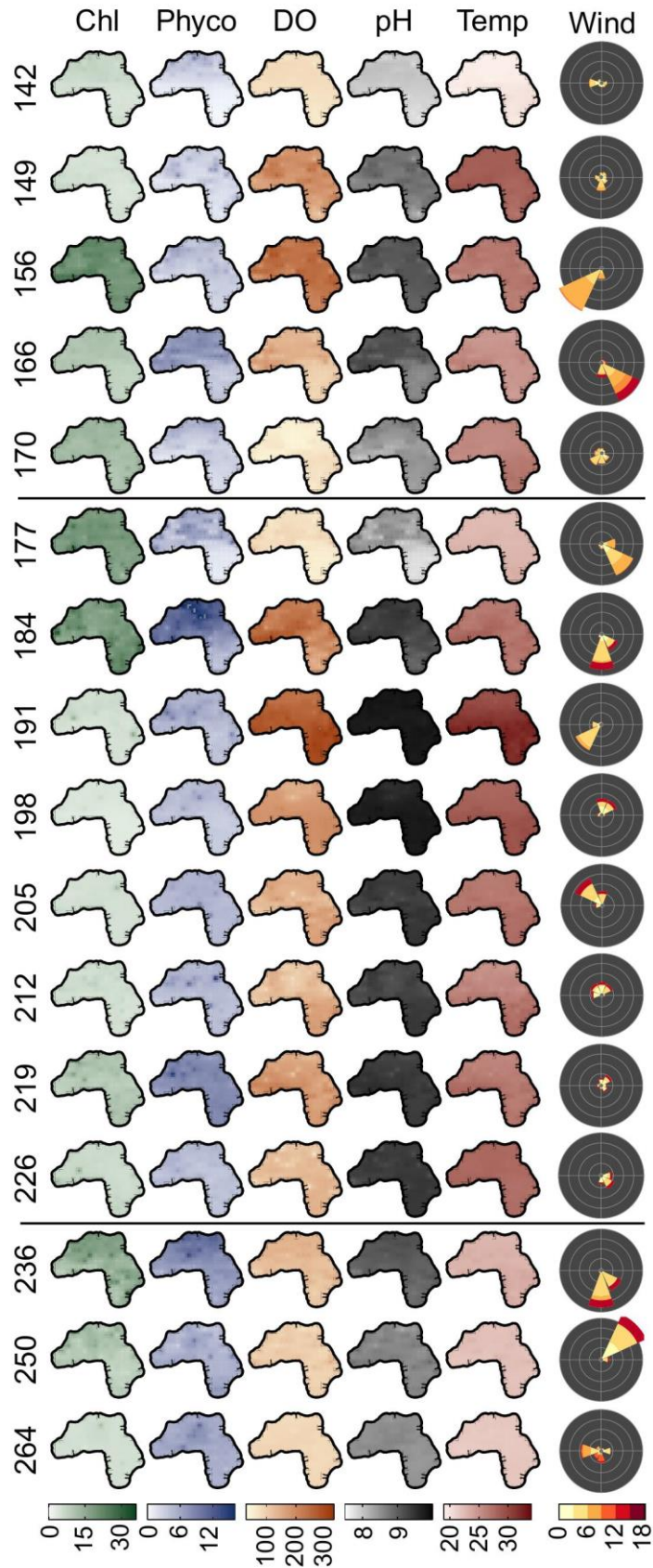
713 Wilkinson, G. M., Carpenter, S. R., Cole, J. J., Pace, M. L., Batt, R. D., Buelo, C. D., &  
714 Kurtzweil, J. T. (2018). Early warning signals precede cyanobacterial blooms in multiple  
715 whole-lake experiments. *Ecological Monographs*, 88(2), 188-203. doi:10.1002/ecm.1286  
716 Wu, X. D., Kong, F. X., Chen, Y. W., Qian, X., Zhang, L. J., Yu, Y., . . . Xing, P. (2010).  
717 Horizontal distribution and transport processes of bloom-forming *Microcystis* in a large  
718 shallow lake (Taihu, China). *Limnologia*, 40(1), 8-15. doi:10.1016/j.limno.2009.02.001  
719 Wynne, T. T., & Stumpf, R. P. (2015). Spatial and Temporal Patterns in the Seasonal  
720 Distribution of Toxic Cyanobacteria in Western Lake Erie from 2002-2014. *Toxins*, 7(5),  
721 1649-1663. doi:10.3390/toxins7051649  
722 Zhou, Y. T., Obenour, D. R., Scavia, D., Johengen, T. H., & Michalak, A. M. (2013). Spatial and  
723 Temporal Trends in Lake Erie Hypoxia, 1987-2007. *Environmental Science &*  
724 *Technology*, 47(2), 899-905. doi:10.1021/es303401b  
725

## Figures



727 **Figure 1.** Sampling locations on a 65 m square grid of Swan Lake, a 40.5 hectare waterbody in  
 728 western Iowa, USA. The main inlet to the lake and only outlet indicated with arrows. a) The  
 729 location of the macrophyte beds of the two dominant species within the lake are shown on the  
 730 map, with darker shading indicating the regions with the densest vegetation and the location of

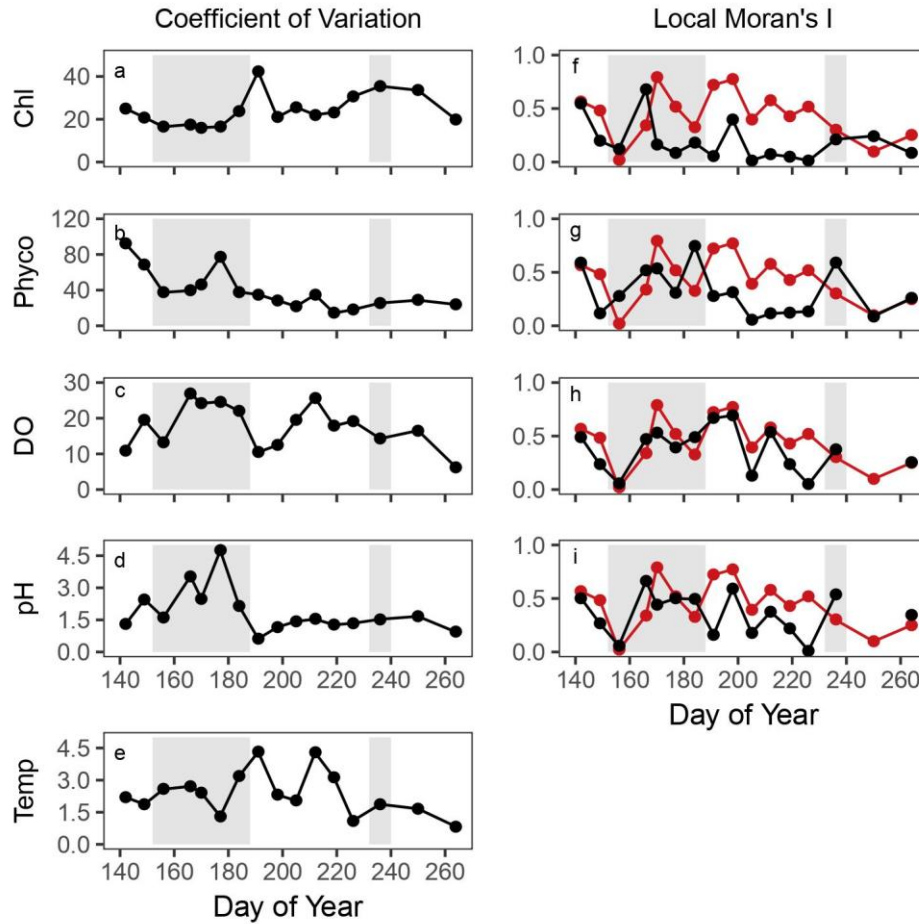
- 731 the high frequency sensor, b) the bathymetry of the lake and location of the lake in the state of  
732 Iowa, in reference to the United States of America.



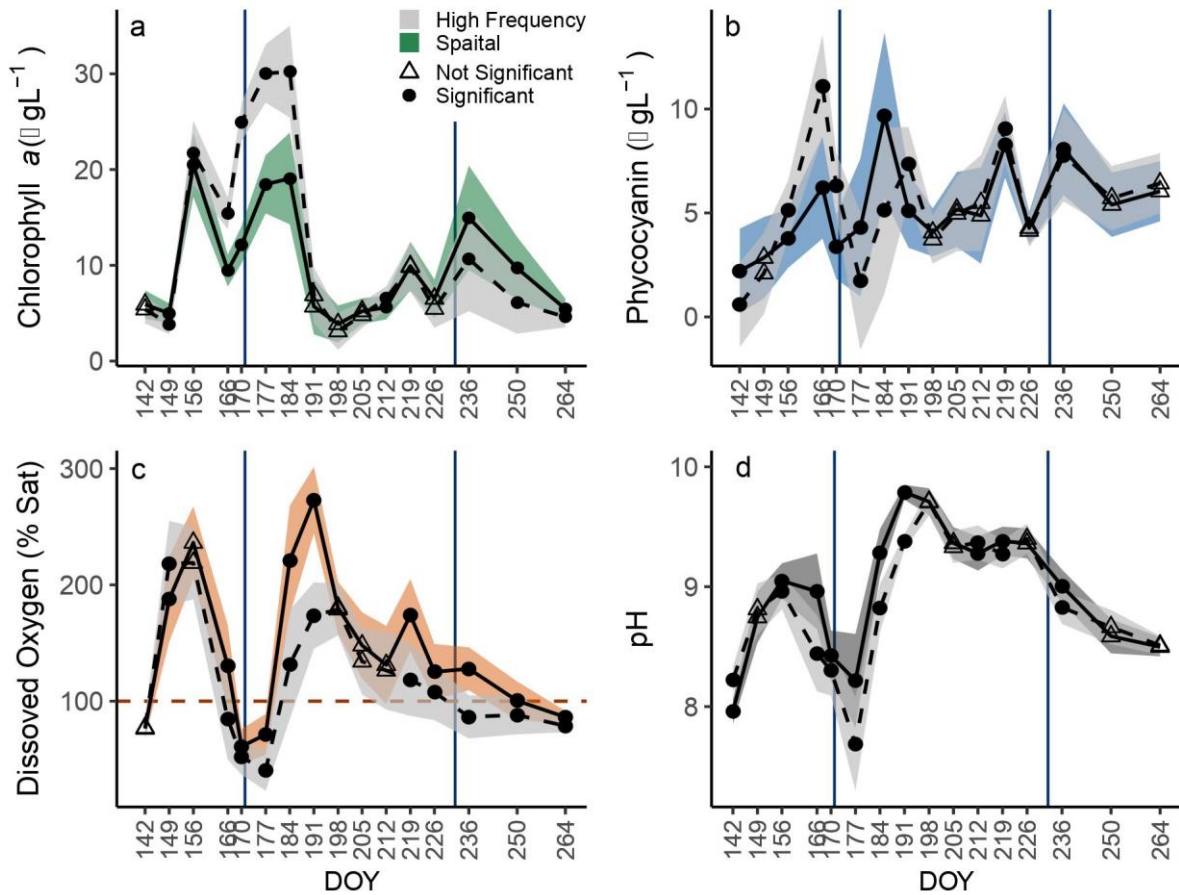
733 **Figure 2.** The spatial pattern of each of the variables chlorophyll *a* (Chl,  $\mu\text{g L}^{-1}$ ), phycocyanin



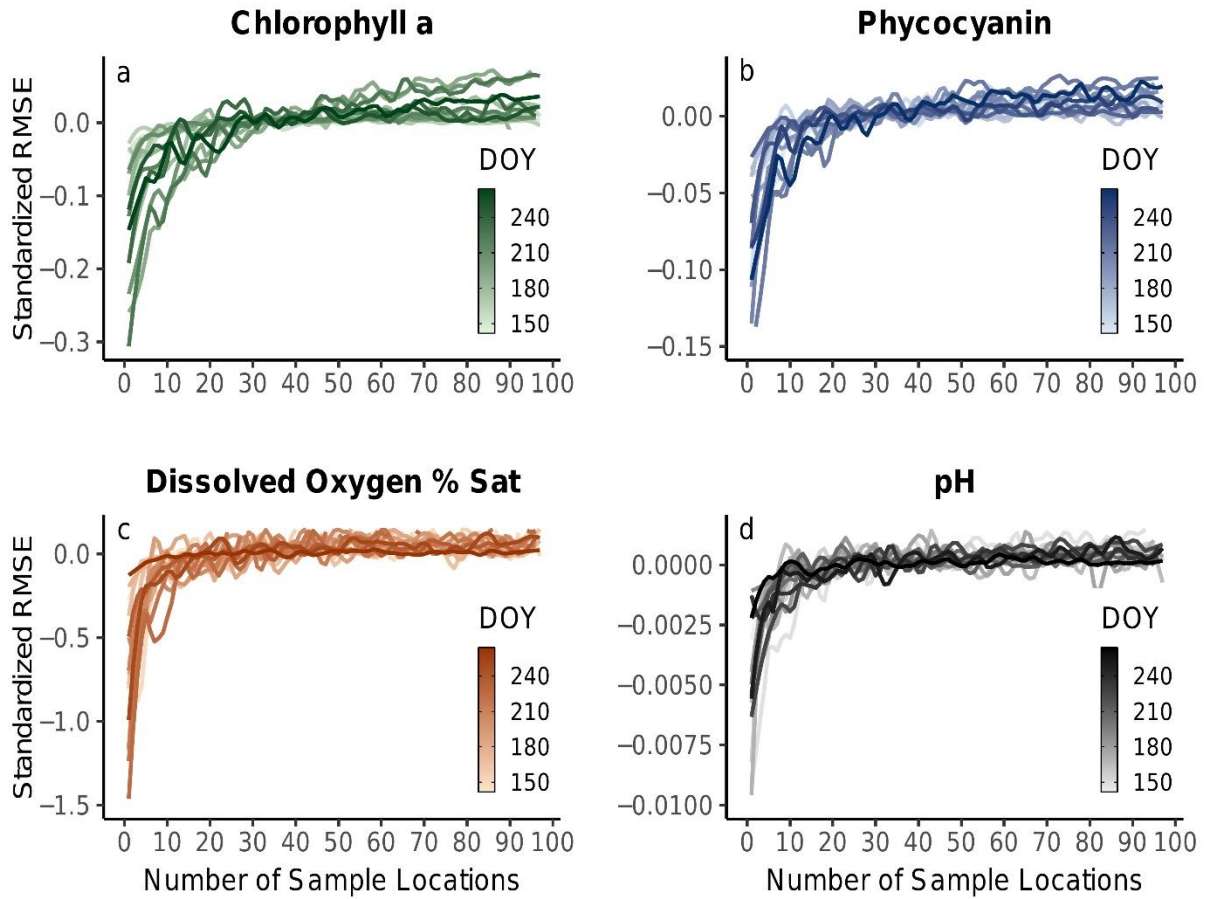
734 (Phyco,  $\mu\text{g L}^{-1}$ ), dissolved oxygen (DO, percent saturation), pH, and temperature (Temp,  $^{\circ}\text{C}$ ) for  
735 each sampling event. The 98 sampling locations taken in a 65m grid (Figure 1) were interpolated  
736 to a 25m grid using spatial inverse distance interpolation for visualization here. The color ramps  
737 for each variable are scaled from the lowest to the highest value observed over the course of the  
738 season across all sampling locations. The wind roses are the wind speeds ( $\text{m s}^{-1}$ ; color ramp) and  
739 direction the wind came from for the 24 hours prior to a sampling event. The concentric circles  
740 are the frequency of winds from that direction for the 24 hour period (expressed as a percentage,  
741 largest circle is 80% of the time). In the case of a longer “spoke”, the greater amount of time the  
742 wind was from that direction. The horizontal lines between DOY 170 and 177, and DOY 226  
743 and 236 mark the two large precipitation events that occurred between those sampling dates.



744 **Figure 3.** Time series of the spatial coefficient of variation (CV) and spatial autocorrelation (AC;  
 745 local Moran's I) of the biologically-mediated variables in Swan Lake (same variable  
 746 abbreviations as Figure 2). The gray polygons indicate periods of algal bloom. The red line is the  
 747 time series of temperature local Moran's I for comparison.



748 **Figure 4.** Comparison of the mean (lines and points) and range (shaded polygon) of  
 749 measurements from the spatial sampling and fixed station measurements. The fixed station data  
 750 were trimmed to the period that spatial sampling occurred. A filled circle is used for the  
 751 sampling dates when the means from the two sampling approaches were significantly different  
 752 ( $p < 0.05$ ), and an open triangle is used for the sampling dates when the mean of the two  
 753 approaches were not significantly different. The dark blue vertical lines indicate the dates of the  
 754 two major precipitation events and the red dashed line in panel c is at 100% dissolved oxygen  
 755 saturation.



756 **Figure 5.** Standardized root mean squared errors (RMSE) of rarefaction analysis. Fit lines  
 757 represent each sampling dates standardized RMSE (16 in total) and the gradient from light to  
 758 dark indicates first sampling event to last.

759

### Supplementary material for

760 **Title:** Capturing the spatial variability of algal bloom development in a shallow temperate lake

761 **Authors:** Ortiz and Wilkinson

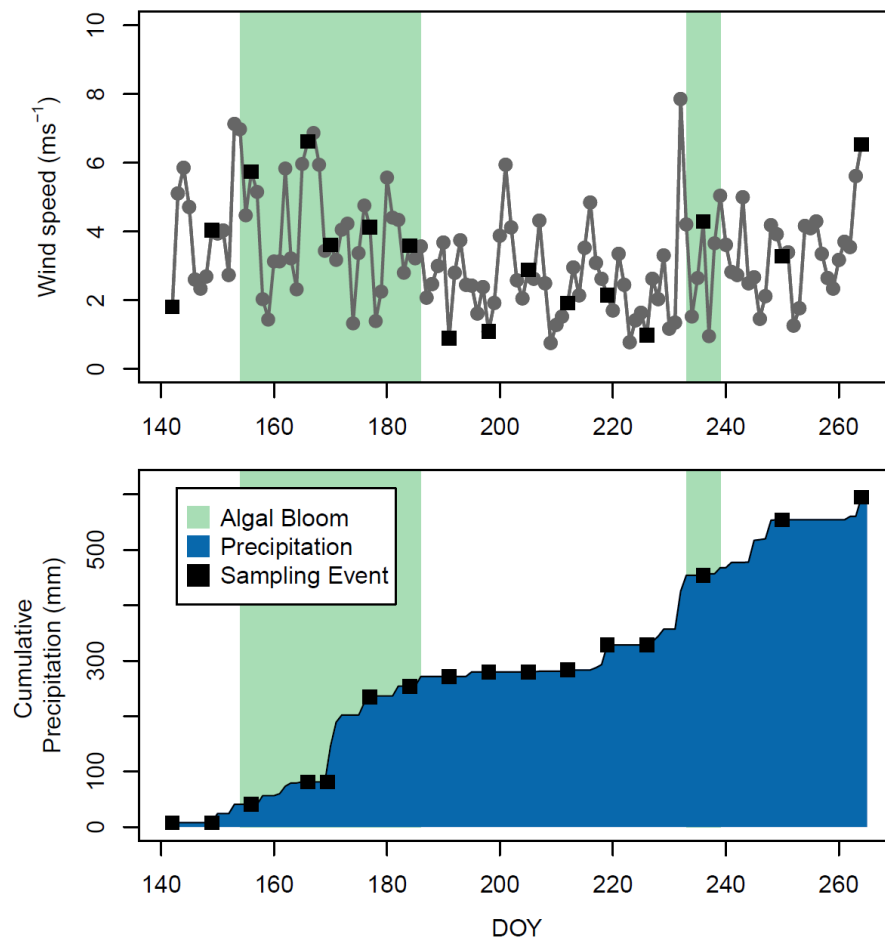
762

763

### Hourly Weather Data

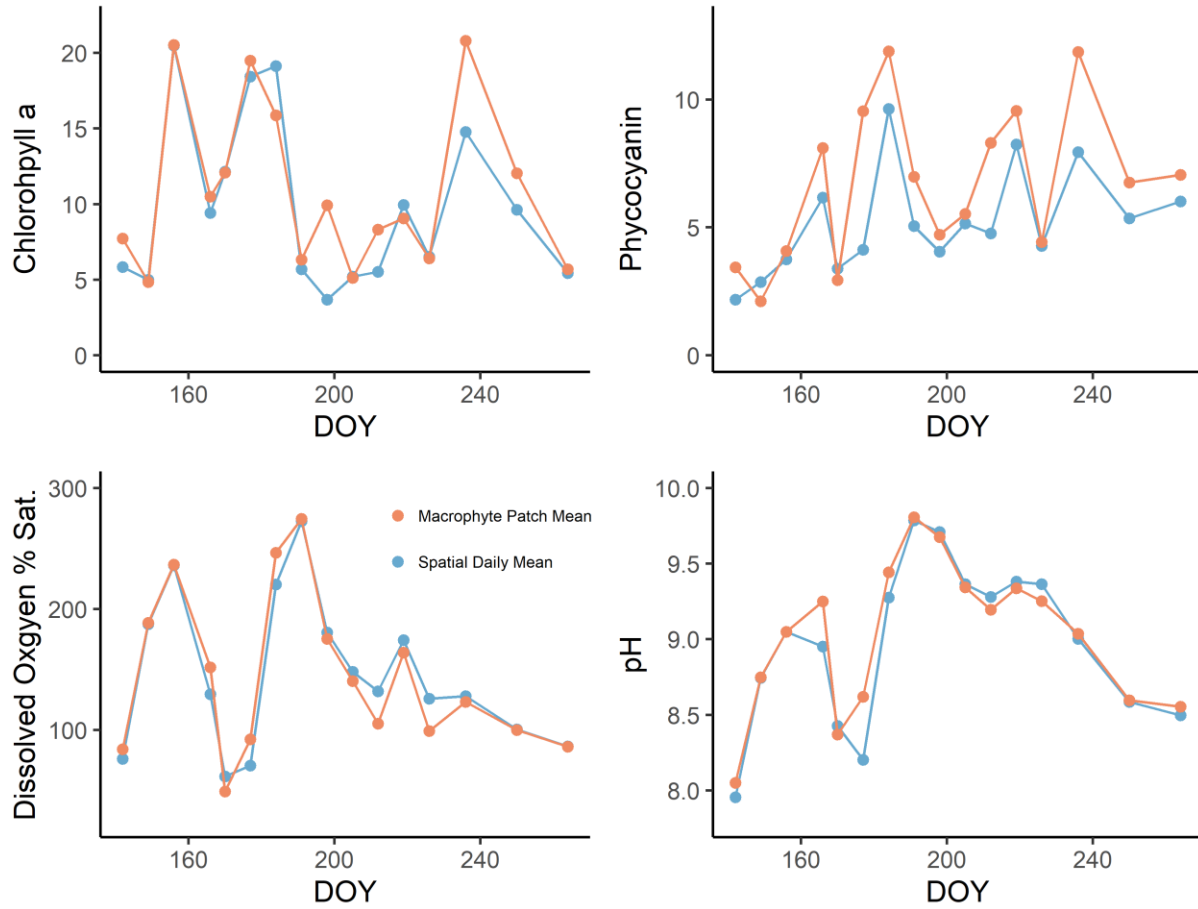
764 Hourly wind and precipitation data were downloaded from the National Oceanic and  
765 Atmospheric Automated Surface Observing System (NOAA ASOS) for Arthur N. Neu Airport  
766 Carroll, Iowa, USA, less than 5km from the lake, through the Iowa State University Iowa  
767 Environmental Mesonet (<https://mesonet.agron.iastate.edu/>). The data were summarized to daily  
768 means and plotted as mean wind speed and cumulative daily precipitation.

769 **Figures**



770

771 **Supplement Figure 1.** Daily meteorological data for the duration of the study. A) Daily mean  
772 wind speed during the study period. Periods of algal bloom in the lake are denoted by the green  
773 polygons. B) The cumulative precipitation from the first to the last day of the study period. There  
774 were two large precipitation events from DOY 170-171 and on DOY 132.



775

776

777

**Supplement Figure 2.** A comparison of the mean value for each variable in the American lotus macrophyte patch (sites C4, D4, D5) and the rest of the lake.